Circulation

ORIGINAL RESEARCH ARTICLE

Phosphorylation-Regulated Dynamic Phase Separation of HIP-55 Protects Against Heart Failure

Yunqi Jiang, PhD*; Jinge Gu, PhD*; Xiaodou Niu, MM*; Jiaojiao Hu, MS; Yongzhen Zhang, PhD; Dan Li, PhD; Yida Tang, PhD; Cong Liu, PhD; Zijian Li, PhD

BACKGROUND: Heart failure (HF), which is the terminal stage of many cardiovascular diseases, is associated with low survival rates and a severe financial burden. The mechanisms, especially the molecular mechanism combined with new theories, underlying the pathogenesis of HF remain elusive. We demonstrate that phosphorylation-regulated dynamic liquid–liquid phase separation of HIP-55 (hematopoietic progenitor kinase 1–interacting protein of 55 kDa) protects against HF.

METHODS: Fluorescence recovery after photobleaching assay, differential interference contrast analysis, pull-down assay, immunofluorescence, and immunohistochemical analysis were used to investigate the liquid–liquid phase separation capacity of HIP-55 and its dynamic regulation in vivo and in vitro. Mice with genetic deletion of HIP-55 and mice with cardiac-specific overexpression of HIP-55 were used to examine the role of HIP-55 on β-adrenergic receptor hyperactivation-induced HF. Mutation analysis and mice with specific phospho-resistant site mutagenesis were used to identify the role of phosphorylation-regulated dynamic liquid–liquid phase separation of HIP-55 in HF.

RESULTS: Genetic deletion of HIP-55 aggravated HF, whereas cardiac-specific overexpression of HIP-55 significantly alleviated HF in vivo. HIP-55 possesses a strong capacity for phase separation. Phase separation of HIP-55 is dynamically regulated by AKT-mediated phosphorylation at S269 and T291 sites, failure of which leads to impairment of HIP-55 dynamic phase separation by formation of abnormal aggregation. Prolonged sympathetic hyperactivation stress induced decreased phosphorylation of HIP-55 S269 and T291, dysregulated phase separation, and subsequent aggregate formation of HIP55. Moreover, we demonstrated the important role of dynamic phase separation of HIP-55 in inhibiting hyperactivation of the β-adrenergic receptor–mediated P38/MAPK (mitogen-activated protein kinase) signaling pathway. A phosphorylation-deficient HIP-55 mutation, which undergoes massive phase separation and forms insoluble aggregates, loses the protective activity against HF.

CONCLUSIONS: Our work reveals that the phosphorylation-regulated dynamic phase separation of HIP-55 protects against sympathetic/adrenergic system–mediated heart failure.

Key Words: beta-adrenergic receptor ■ heart failure ■ phase separation ■ phosphorylation

Heart failure (HF) is the end stage of various cardiovascular diseases, and is associated with high morbidity and mortality rates. The 5-year survival rate is ≈45.5%[1]: lower than that of most malignant tumors. Chronic HF is often characterized by a high risk of recurrence and readmission, which significantly increases the economic burden. Therefore, it is important to understand the pathological mechanisms of worsening prognosis of HF.

Sympathetic activity is essential for maintaining normal cardiac physiological functions and for responding

Correspondence to: Zijian Li, PhD, Peking University Third Hospital, Huayuan North Rd, Number 49, Haidian District, 100191, Beijing, China, Email lizijian@bjmu.edu.cn; or Cong Liu, PhD, Interdisciplinary Research Center on Biology and Chemistry, Shanghai Institute of Organic Chemistry, Chinese Academy of Sciences, Haike Rd, Number 100, 201210, Shanghai, China, Email liulab@sioc.ac.cn
*Y. Jiang, J. Gu, and X. Niu contributed equally.
Supplemental Material is available at https://www.ahajournals.org/doi/suppl/10.1161/CIRCULATIONAHA.123.067519.
For Sources of Funding and Disclosures, see page 951.

Circulation is available at www.ahajournals.org/journal/circ

Clinical Perspective

What Is New?

- The sympathetic-adrenergic system can dynamically induce cardiac protein liquid–liquid phase separation.
- The authors directly link pathological stimuli–induced dysregulation of protein phase separation to heart failure.
- HIP-55 (hematopoietic progenitor kinase 1–interacting protein of 55 kDa) protects against heart failure dependent on its dynamic phase separation, providing a new strategy for treatment.

What Are the Clinical Implications?

- Targeting the phase separation of HIP-55 may provide a new strategy for drug development for heart failure treatment.

Nonstandard Abbreviations and Acronyms

β-AR	β-adrenergic receptor
ERK	extracellular signal-regulated protein kinase
FUS	fused in sarcoma
HF	heart failure
HIP-55	hematopoietic progenitor kinase 1–interacting protein of 55 kDa
hnRNPA1	heterogeneous nuclear ribonucleoprotein A1
LCD	low-complexity domain
LLPS	liquid–liquid phase separation
MAPK	mitogen-activated protein kinase
SH3	Src homology 3
TDP-43	TAR DNA-binding protein 43
WT	wild-type

to sudden stimuli, such as fight-or-flight response.[2] However, prolonged overactivation of the sympathetic system plays a key role in HF.[2,3] Sympathetic system overactivation leads to dysfunction of β-adrenergic receptors (β-ARs) and downstream signaling of P38/MAPK (mitogen-activated protein kinase), ERK (extracellular signal-regulated protein kinase)/MAPK, and AKT, among others.[3–6] A majority of our knowledge on the mechanisms underlying HF is derived from classic receptor signal transduction theory. However, β-ARs possess a Janus-faced nature under physiological and pathological conditions. That is, β-ARs and downstream signaling can mediate both normal cardiac physiological functions and HF. Classic receptor signal transduction theory has difficulty explaining how the same receptor and downstream signaling system can switch between normal physiology and HF. Therefore, it is necessary to uncover the dynamic switch mechanism between physiology and pathology, and identify its key molecular switch contributing to HF.

Recent studies have emphasized the dual role of protein liquid–liquid phase separation (LLPS) under both normal physiological and pathological conditions.[7] LLPS is a process during which proteins shift from a scattered to clustered state, aiding in various essential biological actions, such as signaling transduction, enzymatic reactions, and gene transcription, among others.[7–10] The LLPS process is intricately regulated by posttranslational modifications, protein–protein interactions, and other factors.[7–10] Disturbances in this system can lead to severe illness, including neurological disorders and cancer.[11] However, the role of LLPS in cardiovascular diseases remains unclear.

In our previous research, we used a proteomic approach to reveal a novel β-AR regulator protein HIP-55 (hematopoietic progenitor kinase 1–interacting protein of 55 kDa) in cardiac remodeling.[5] HIP-55 can negatively regulate receptor downstream signaling.[5] As a multidomain adaptor protein, HIP-55 possesses an actin-binding domain at its N-terminus and an SH3 (Src homology 3) domain at its C-terminus.[12] Through these domains, HIP-55 is able to interact with several critical signaling molecules, including F-actin, MAP4K1 kinase, and Src kinase, to trigger cellular responses such as endocytosis, proliferation, and cell survival.[12,13] Furthermore, we found a low-complexity domain (LCD) situated within the HIP-55 middle region through structural analysis. An LCD has been shown to be the structure basis for LLPS. Thus, we reasoned that HIP-55 may function by means of LLPS.

In this study, we demonstrate that phosphorylation-regulated dynamic phase separation of HIP-55 protects against β-AR–mediated HF. Furthermore, we found that HIP-55 possesses a strong capacity for phase separation, regulated by AKT-mediated phosphorylation at S269 and T291. Prolonged sympathetic stress induced decreased HIP-55 S269/T291 phosphorylation and dysregulated phase separation, causing subsequent aggregate formation of HIP-55. In line with this mechanism, cardiac-specific overexpression of phosphorylation-deficient S269A/T291A-mutated HIP-55, which tends to form massive dysregulated granules and insoluble aggregates, fails to inhibit the progression of HF. Our findings not only connect prolonged sympathetic overactivation and dysregulated phase separation to HF but also hint at the potential for therapeutic targeting of the regulated phase separation of HIP-55.

METHODS

The data, all protocols, and study materials will be made available to other researchers for purposes of reproducing the results or replicating the procedures. Detailed descriptions

of experimental methods are provided in the Supplemental Material.

Experimental Animals

All experiments involving animals were approved by the biomedical research ethics committee of Peking University and are compliant with the National Institutes of Health Guide for the Care and Use of Laboratory Animals.

Statistical Analysis

GraphPad Prism version 8.0 (GraphPad Software) was used for all statistical analyses. Data are given as mean±SEM. Data were first tested for normality. Data with normal distribution were analyzed by unpaired 2-tailed Student *t* test (for 2 groups). For comparisons among multiple groups, 1-way or 2-way ANOVA was performed, followed by Bonferroni post hoc correction. Otherwise, nonparametric statistical analyses were performed using the Mann-Whitney *U* test for 2 groups or the Kruskal-Wallis test followed by the Dunn post hoc test for multiple comparisons (≥3 groups). Differences between groups were considered significant at $P<0.05$.

RESULTS

Genetic Deletion of HIP-55 Promotes HF

Our previous proteomic study suggested that HIP-55 is involved in the pathological progression of heart adverse remodeling.[5] We therefore sought to examine the biological functions of HIP-55 in HF. HIP-55 knockout (HIP-55$^{-/-}$) mice were generated and characterized (Figure 1A and 1B). The HIP-55$^{-/-}$ mice and control wild-type (WT) mice were subjected to long-term isoproterenol treatment to induce HF. Echocardiography analysis demonstrated significantly aggravated cardiac dysfunction in HIP-55 deficiency mice compared with WT mice after the long-term sympathetic hyperactivation (Figure 1C; Table S1). Moreover, HIP-55 deficiency dramatically increased cardiac hypertrophy after administration of isoproterenol as demonstrated by heart weight/tibia length and cardiomyocyte cross-sectional area analysis (Figure 1D through 1F). Sirius red staining also revealed that myocardial fibrosis was obviously increased in HIP-55$^{-/-}$ mice compared with the controls (Figure 1G). Furthermore, cardiac dysfunction marker gene expression, including *ANP*, *BNP*, and *MHC* isoform switch, were promoted in the hearts of HIP-55$^{-/-}$ mice (Figure 1H). These results showed that the presence of HIP-55 protects against HF after long-term sympathetic hyperactivation.

Cardiac-Specific Overexpression of HIP-55 Alleviates HF

To further investigate the cardiac-specific role of HIP-55, we constructed cardiac-specific HIP-55–overexpressing (HIP-55^{Tg}) mice (Figure 2A and 2B). HIP-55^{Tg} and control mice underwent isoproterenol-induced HF, as described previously. Compared with control mice, cardiac function was significantly better in HIP-55^{Tg} mice after isoproterenol treatment (Figure 2C; Table S2). Moreover, the HIP-55^{Tg} mice exhibited largely diminished isoproterenol-induced cardiac hypertrophy compared with WT mice (Figure 2D through 2F). Sirius staining also revealed that myocardial fibrosis was significantly decreased in HIP-55^{Tg} mice compared with controls (Figure 2G). In addition, the cardiac dysfunction marker genes were also suppressed in HIP-55^{Tg} mouse heart tissues compared with controls (Figure 2H). These results showed that cardiac-specific overexpression of HIP-55 significantly protected against HF progression.

HIP-55 Undergoes Phase Separation in Vitro and in Cells

We next sought to detect the cellular localization and distribution of HIP-55 in cells. mCherry-tagged HIP-55 forms granule-like structures in cytoplasm of NIH-3T3 cells (Figure 3A). We further observed that the small HIP-55 granule-like puncta can dynamically fuse together into larger granules in living NIH-3T3 cells (Figure 3B). Moreover, by performing a fluorescence recovery after photobleaching assay, we found that the quenched fluorescence signal of HIP-55 in granule-like structures recovers rapidly, in about 20 seconds. However, it can only recover to ≈65% (Figure 3C). These data demonstrate that HIP-55 forms granule-like structures in cells with moderate internal dynamic properties.

We then examined whether HIP-55 exhibits intrinsic capability for phase separation. Recombinant HIP-55 protein was purified in vitro with high purity. We found that HIP-55 displayed a high capacity to phase separate and could form spherical droplets in the presence of different crowding reagents, including Ficoll, dextran, and polyethylene glycol (Figure 3D), which are commonly used to mimic a cellular crowding environment.[14] The small HIP-55 droplets can spontaneously fuse together upon contact (Figure 3E). Fluorescence recovery after photobleaching analysis showed that the quenched fluorescence signal of HIP-55 in droplets could recover up to ≈80% in 100 seconds (Figure 3F). Together, these results demonstrate that HIP-55 has a strong ability to phase separate.

Intrinsically Disordered LCD Mediates Phase Separation of HIP-55

We next sought to investigate the molecular basis underlying HIP-55 phase separation. We prepared 3 different truncations of HIP-55, targeting the actin-depolymerizing factor homology domain (residues 1–140), the LCD (residues 141–373), or the SH3

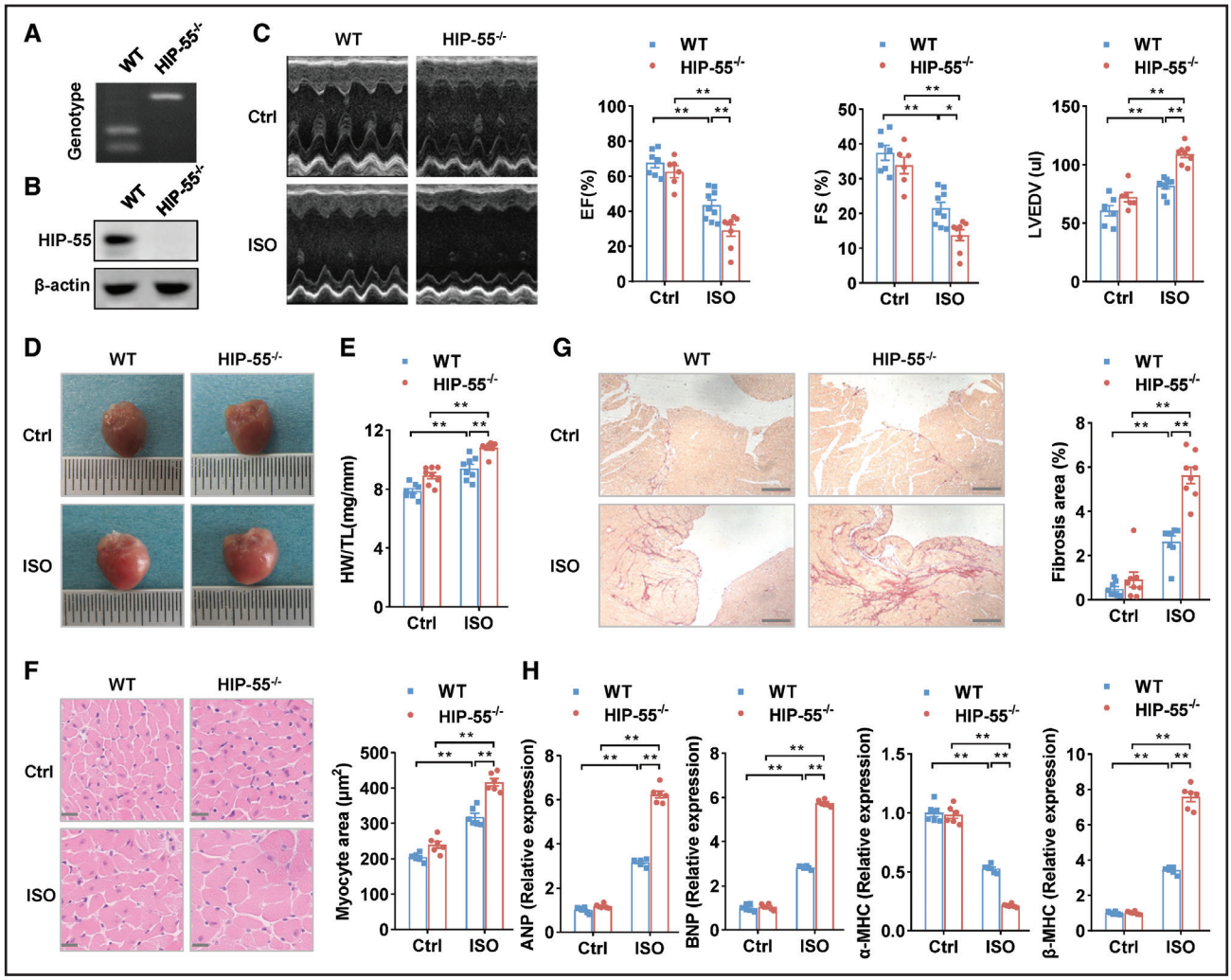

Figure 1. Genetic deletion of HIP-55 promotes heart failure.
A, Genotypes of wild-type (WT) and HIP-55$^{-/-}$ mice. **B**, Western blot analysis of HIP-55 (hematopoietic progenitor kinase 1–interacting protein of 55 kDa) expression in WT and HIP-55$^{-/-}$ mouse heart tissue. **C**, Deletion of HIP-55 promoted isoproterenol (ISO)–induced heart failure. Representative echocardiographic imaging and analysis of ejection fraction (EF%), fractional shortening (FS%), and left ventricular end diastolic volume (LVEDV) after continuous administration of saline or ISO with minipumps for 4 weeks (n=6–9). **D**, Deletion of HIP-55 promoted ISO-induced adverse cardiac remodeling. Representative gross heart photographs of control and HIP-55$^{-/-}$ mice after saline or ISO administration. **E**, The ratio of heart weight to tibial length (HW/TL; n=8). **F**, Hematoxylin & eosin staining micrographs of cross-sections of myocardium (n=6). Scale bar=20 μm. **G**, Deletion of HIP-55 promoted ISO-induced adverse cardiac fibrosis. The fibrotic area was quantified as the ratio of Sirius red staining area to total area of cross-sectional tissue (n=8). Scale bar=250 μm. **H**, mRNA levels of heart failure marker genes *ANP*, *BNP*, *α-MHC*, and *β-MHC* in HIP-55$^{-/-}$ and WT mice after ISO treatment (n=6). Statistical analyses were performed by 2-way ANOVA followed by Bonferroni post hoc correction (**C**, **E**, **F**, **G**, and **H**). **P*<0.05, ***P*<0.01.

domain (residues 374–430; Figure 4A). As revealed by the differential interference contrast and turbidity assay, only the LCD, but not the other 2 domains, could spontaneously form liquid-like droplets in the presence of polyethylene glycol, which recapitulates the phase separation behavior of full-length HIP-55 (Figure 4B), implying the essential role of the LCD in mediating HIP-55 phase separation. Bioinformatic prediction further showed that the majority of the LCD displays an intrinsically disordered conformation (Figure 4A), which is consistent with previous studies showing that intrinsically disordered regions have a high propensity for mediating protein phase separation.[15]

To further pinpoint the key residues within the LCD for mediating HIP-55 phase separation, we performed amino acid composition analysis of the LCD. The LCD features a typical low-complex sequence, which contains a high proportion of glutamate (E), glutamine (Q), arginine (R), and alanine (A; Figure 4C and 4D). More than 25% of the total amino acids of the LCD are composed of charged residues, including negatively charged Glu and positively charged Arg, which are widely distributed throughout the LCD. This strongly suggests that electrostatic interactions are important in mediating HIP-55 phase separation. Because high salt concentration can potentially impair charged interactions, we tested the

ORIGINAL RESEARCH ARTICLE

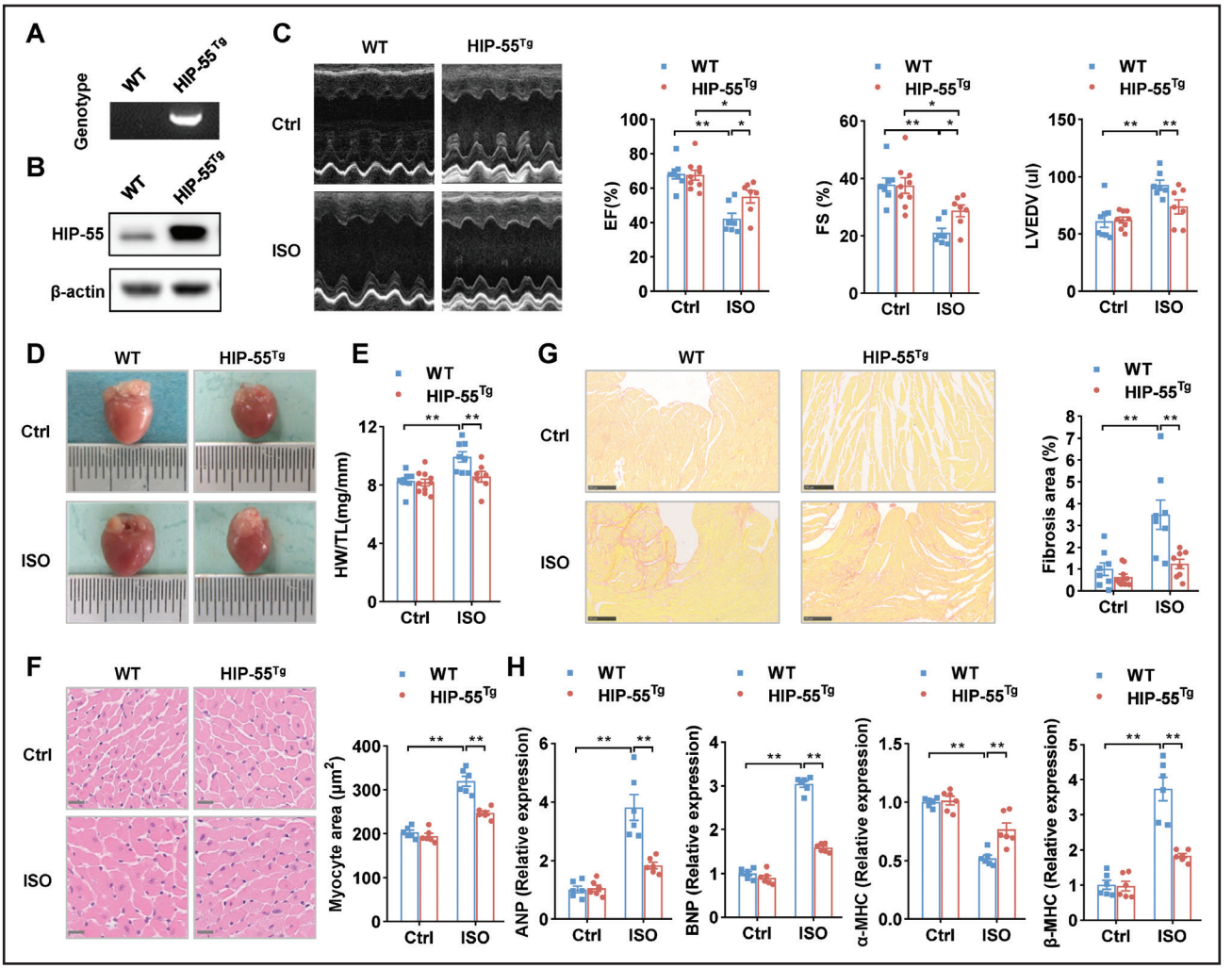

Figure 2. Cardiac-specific overexpression of HIP-55 alleviates heart failure.
A, Genotypes of wild-type (WT) and HIP-55^{Tg} mice. **B**, Detection of HIP-55 (hematopoietic progenitor kinase 1–interacting protein of 55 kDa) expression in heart tissue from WT and HIP-55^{Tg} mice by Western blot. **C**, Cardiac-specific overexpression of HIP-55 alleviated isoproterenol (ISO)–induced heart failure. Representative M-mode echocardiographic imaging of heart and cardiac function analysis of ejection fraction (EF%), fractional shortening (FS%), and left ventricular end diastolic volume (LVEDV) after 4 weeks of ISO treatment (n=7–9). **D**, Cardiac-specific overexpression of HIP-55 inhibited ISO-induced adverse cardiac remodeling. Representative gross heart photographs of control and HIP-55^{Tg} mice after saline or ISO administration. **E**, Heart weight/tibial length (HW/TL) ratios (n=7–10). **F**, Micrographs of hematoxylin & eosin–stained myocardium cross-sections. Scale bar=20 μm (n=6). **G**, Cardiac-specific overexpression of HIP-55 inhibited ISO-induced adverse cardiac fibrosis. Representative images of heart sections stained with Sirius red staining and statistical results (n=8–10). Scale bar=250 μm. **H**, mRNA levels of heart failure marker genes expression (*ANP*, *BNP*, *α-MHC*, and *β-MHC*) in HIP-55^{Tg} and WT mice after ISO treatment (n=6). Statistical analyses were performed by 2-way ANOVA followed by Bonferroni post hoc correction (**C**, **E**, **F**, **G**, and **H**). **P*<0.05, ***P*<0.01.

effect of salt on HIP-55 LLPS. In line with expectations, increasing the concentration of NaCl in the buffer gradually impaired phase separation of HIP-55 (Figure 4E).

To validate the role of the charged residues of the LCD in HIP-55 phase separation, we mutated 22 Arg residues in the LCD to Ala (termed HIP-55R/A) and examined its phase separation both in vitro and in cells. Differential interference contrast and turbidity measurements showed that the R/A mutant eliminated the phase separation capability of HIP-55 under the tested in vitro conditions (Figure 4F). Moreover, compared with WT HIP-55 (HIP-55WT), HIP-55R/A formed significantly fewer granule-like structures (Figure 4G). Taken together, our data demonstrate that the charged residues in the LCD drive phase separation of HIP-55 by means of electrostatic interactions both in vitro and in cells.

Phosphorylation of S269/T291 Within LCD Regulates HIP-55 Phase Separation

We further sought to explore the dynamic regulation of HIP-55 phase separation and its potential role in HF progression. We previously demonstrated that AKT, a key participant in HF,[3] can directly phosphorylate HIP-55. The AKT phosphorylation sites S269 and T291 are both localized to the HIP-55 LCD (residues 141–373).

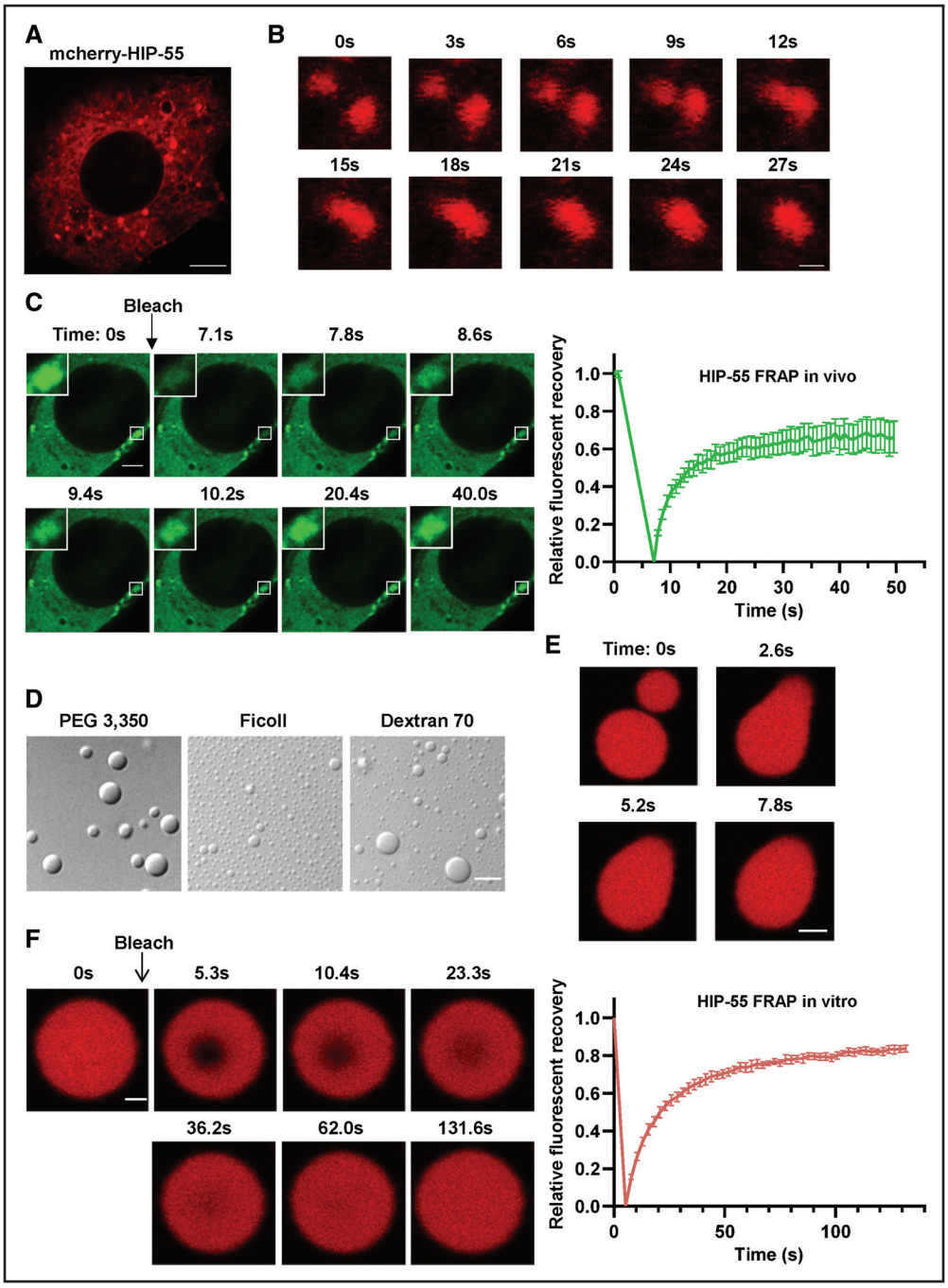

Figure 3. HIP-55 undergoes phase separation in vitro and in cells.
A, A representative confocal image shows that overexpressed mCherry–HIP-55 (hematopoietic progenitor kinase 1–interacting protein of 55 kDa) massively forms puncta in NIH-3T3 cells. Scale bar=5 μm. **B**, Representative images show the fusion process of 2 HIP-55 granules in a living NIH-3T3 cell. Scale bar=1 μm. **C**, Representative images and fluorescence recovery after photobleaching (FRAP) curve of HIP-55 granules in NIH-3T3 cells. The black arrow indicates the action of photobleaching. Scale bar=2.5 μm (n=10). **D**, Differential interference contrast images of 50 μM HIP-55 under 100 mM NaCl (pH 7.5) and different 10% polymers as indicated. Scale bar=5 μm. **E**, Fusion of 2 HIP-55 droplets. Scale bar=2 μm. **F**, FRAP measurement of HIP-55 droplets in 50 μM HIP-55, 100 mM NaCl (pH 7.5), and 10% polyethylene glycol (PEG) 3350. Confocal images show the FRAP process of a droplet. The black arrow indicates the action of photobleaching. The graph shows the FRAP curve of HIP-55 droplets (n=6). Scale bar=1 μm.

Because phosphorylation can effectively alter protein electrostatic interactions, which has been widely observed for regulating protein phase separation,[15] we examined whether S269/T291 phosphorylation is important in modulating HIP-55 phase separation. When co-expressed with constitutively active AKT ($AKT_{\Delta PH}$), HIP-55 was remarkably phosphorylated at both S269 and T291 sites (Figure 5A). The number of HIP-55 granules

ORIGINAL RESEARCH ARTICLE

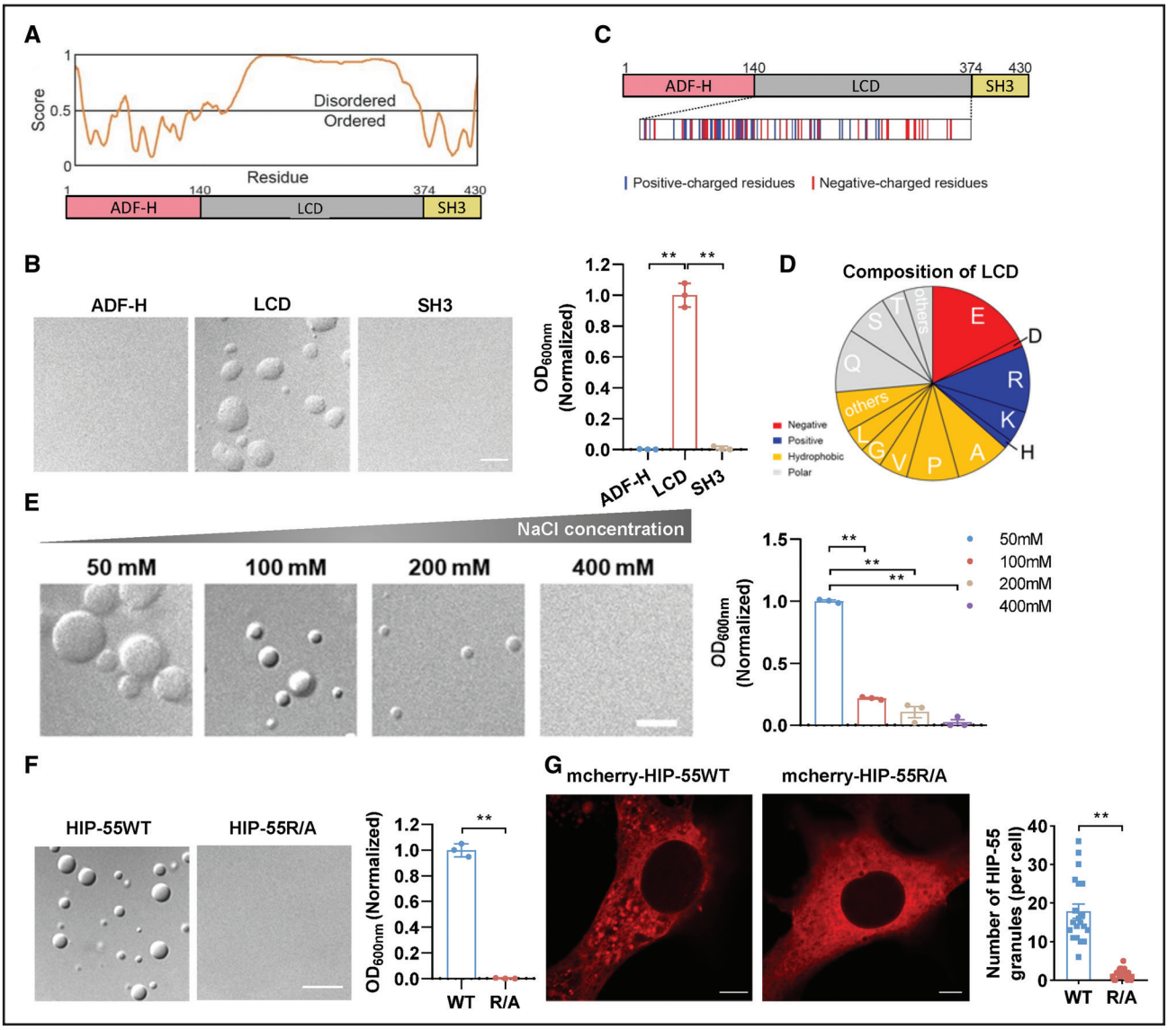

Figure 4. The intrinsically disordered low-complexity domain mediates phase separation of HIP-55.
A, Graph plotting the intrinsically disordered region of HIP-55 (hematopoietic progenitor kinase 1–interacting protein of 55 kDa) proteins using predictor of natural disordered regions with the VSL2 algorithm (**top**) and its domain architecture (**bottom**). **B**, Differential interference contrast images and turbidity measurement of HIP-55WT and its variants using 50 μM protein, 100 mM NaCl (pH 7.5), and 10% polyethylene glycol 3350 (n=3). Scale bar=5 μm. **C**, Different colored bands display the amount and distribution of different types of residues within the low-complexity domain (LCD). **D**, The proportion of abundant amino acid residues in LCD. **E**, Differential interference contrast images and turbidity measurements of 30 μM HIP-55 at pH 7.5 and 10% polyethylene glycol 3350 with indicated concentrations of NaCl (n=3). Scale bar=5 μm. **F**, Differential interference contrast images and turbidity measurements of HIP-55WT and R/A using 50 μM protein, 100 mM NaCl (pH 7.5), and 10% polyethylene glycol 3350 (n=3). Scale bar=10 μm. **G**, Confocal images show NIH-3T3 cells expressing mCherry-tagged HIP-55 WT or R/A (**left**). The graph (**right**) shows the analysis of the HIP-55 granules per cell expressing HIP-55 WT or R/A (n=20). Scale bar=5 μm. Statistical analyses were performed by 1-way ANOVA followed by Bonferroni post hoc correction (**B** and **E**), unpaired *t* test (**F**), and Mann-Whitney *U* test (**G**). ***P*<0.01. ADF-H indicates actin-depolymerization factor homology; and SH3, Src homology 3.

was significantly diminished (Figure 5B). In contrast, either siRNA knockdown of AKT or treatment with the specific AKT kinase inhibitor MK-2206 promoted the formation of HIP-55 granules in cells (Figure 5C through 5E).

To directly examine the effect of AKT phosphorylation on HIP-55 phase separation, we conducted an in vitro phosphorylation assay. Phosphorylation of HIP-55 by AKT almost abolished phase separation of HIP-55 (Figure 5F and 5G). Because AKT directly phosphorylated HIP-55 at S269 and T291 (Figure 5F), we further mutated the 2 AKT-phosphorylation residues including S269 and T291 to aspartate (D) to mimic phosphorylation (HIP-55DD). Compared with HIP-55WT, HIP-55DD exhibited a greatly weakened capacity for phase separation (Figure 5H). In addition, we mutated S269 and T291 to alanine (HIP-55AA) to create an AKT phosphorylation-deficient mutation. Compared with HIP-55WT, treatment of AKT did not alter phase separation of HIP-55AA (Figure 5I and 5J),

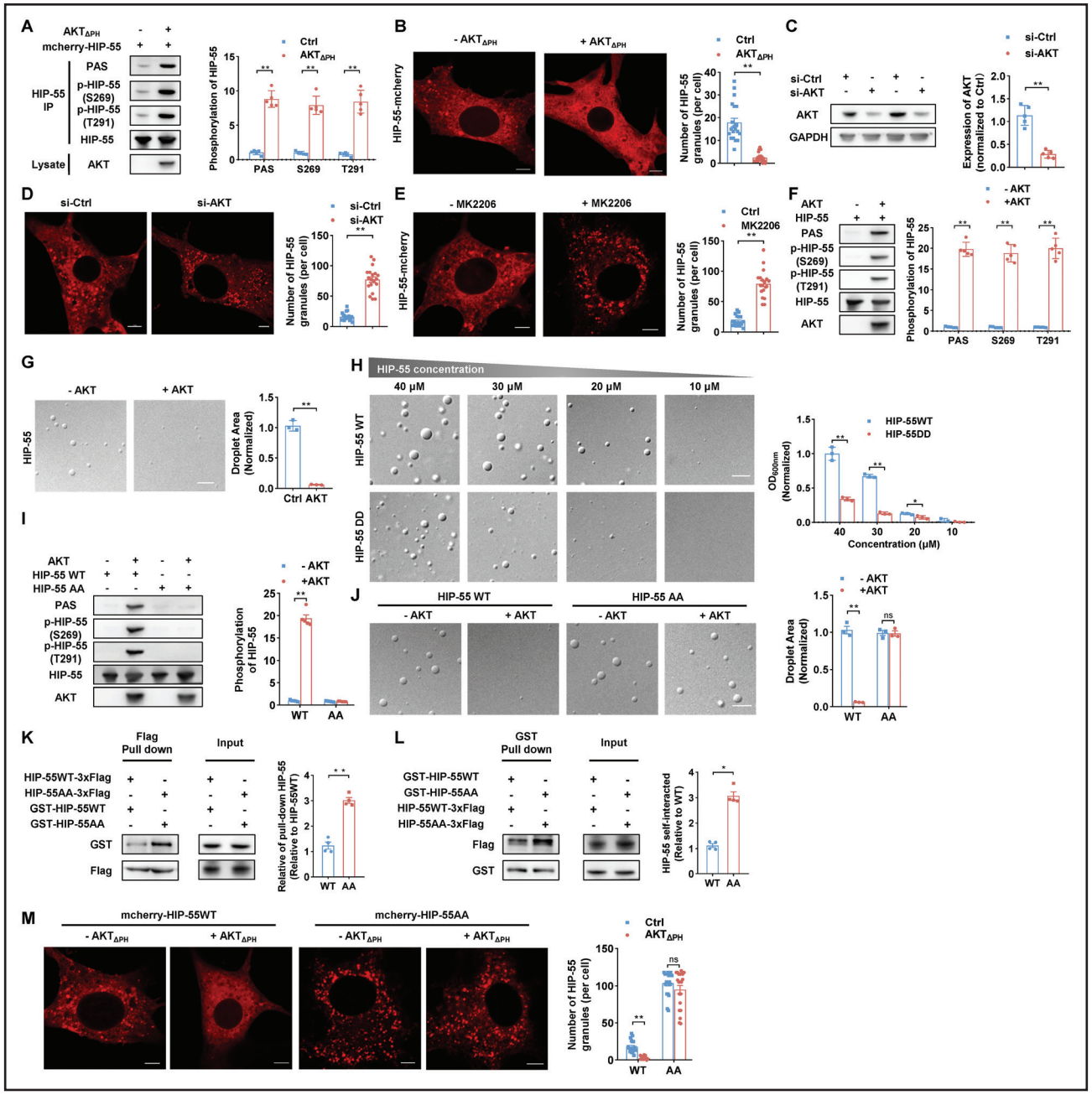

Figure 5. Phosphorylation of S269/T291 within the low-complexity domain regulates HIP-55 phase separation.
A, AKT phosphorylated HIP-55 (hematopoietic progenitor kinase 1–interacting protein of 55 kDa) in vivo. Cells were transfected with mCherry–HIP-55 or constitutively active AKT ($AKT_{\Delta PH}$) plasmids as indicated. mCherry–HIP-55 was enriched by HIP-55 immunoprecipitation and then detected by specific antibodies recognizing phospho-AKT substrate (PAS), p-HIP-55 (S269), or p-HIP-55 (T291; n=5). **B**, NIH-3T3 cells were transfected with mCherry-tagged HIP-55 or $AKT_{\Delta PH}$ plasmids as indicated. Representative confocal image (**left**) and quantification of HIP-55 granules (**right**; n=20). Scale bar=5 μm. **C**, NIH-3T3 cells were transfected with small interfering RNA (siRNA) to knock down AKT. The knockdown efficiency of AKT in NIH-3T3 cells was verified using Western blot analysis (n=5). **D**, NIH-3T3 cells were transfected with mCherry–HIP-55 plasmids and indicated siRNA. Representative confocal image (**left**) and quantification of HIP-55 granules (**right**; n=20). Scale bar=5 μm. **E**, NIH-3T3 cells were transfected with mCherry–HIP-55 plasmids and treated with the specific AKT kinase inhibitor MK2206 (5 μM for 48 hours). Representative confocal image (**left**) and quantification of HIP-55 granules (**right**; n=20). Scale bar=5 μm. **F**, AKT directly phosphorylated HIP-55. Purified recombinant HIP-55 was incubated with active AKT kinase and measured using an in vitro kinase assay. Phosphorylated HIP-55 was detected by PAS, p-HIP-55 (S269), or p-HIP-55 (T291) antibodies (n=5). **G**, Phosphorylation of HIP-55 by AKT abolished phase separation of HIP-55. Differential interference contrast images show HIP-55 in liquid–liquid phase separation (LLPS) condition after incubating with or without AKT for 1 hour. LLPS condition: 20 μM HIP-55 protein, 80 mM NaCl (pH 7.5), and 10% polyethylene glycol (PEG) 3350 (n=3). Scale bar=5 μm. **H**, Differential interference contrast images and LLPS turbidity of HIP-55 WT or DD (S269D/T291D) at the indicated concentration, 100 mM NaCl (pH 7.5), and 10% PEG 3350 (n=3). Scale bar=5 μm. **I**, AKT phosphorylated S269 and T291 residues of HIP-55. Purified recombinant HIP-55WT or HIP-55AA (S269A/T291A) was incubated with active AKT kinase and measured using an in vitro kinase assay, and then the phosphorylated HIP-55 was detected by PAS, p-HIP-55 (S269), or p-HIP-55 (T291) antibodies. (*Continued*)

Figure 5 Continued. The results of PAS were used to quantitatively analyze phosphorylation of HIP-55 (n=5). **J**, Differential interference contrast images showed HIP-55 WT or AA after incubating with or without AKT for 1 hour under LLPS conditions, 20 μM HIP-55 protein, 80 mM NaCl (pH 7.5), and 10% PEG 3350. The graph shows quantitative analysis of droplet area under the aforementioned condition (n=3). Scale bar=5 μm. **K**, HEK293A cells were co-transfected with plasmids as indicated. Cell lysates were immunoprecipitated with anti-Flag beads and then subjected to immunoblotting (n=4). **L**, HEK293A cells were co-transfected with plasmids as indicated. Cell lysates were immunoprecipitated with glutathione-Sepharose 4B beads and then subjected to immunoblotting (n=4). **M**, NIH-3T3 cells were transfected with mCherry-tagged HIP-55 or $AKT_{\Delta PH}$ plasmids as indicated. Representative confocal images (**left**) and quantification of HIP-55 granules (**right**; n=20). Scale bar=5 μm. Statistical analyses were performed by the unpaired *t* test (**C**, **G**, **H**, **J**, and **K**), the Mann-Whitney *U* test (**A**, **B**, **D**, **E**, **F**, **I**, and **L**), and the Kruskal-Wallis test followed by the Dunn post hoc test (**M**). $^{**}P<0.01$.

which strongly supports the notion that phosphorylation of these 2 sites is crucial for reversing phase separation of HIP-55. By using pull-down assays, we further demonstrated that HIP-55AA induced more significant HIP-55 protein self-interactions than did HIP-55WT, suggesting that phosphorylation impairs HIP-55 LLPS by intervening in its self-association (Figure 5K and 5L). In line with in vitro observations and pull-down assays, mCherry-tagged HIP-55AA exhibited a pronounced tendency to phase separate compared with HIP-55WT, which was not diminished by co-expression of constitutively active AKT (Figure 5M). Taken together, our results demonstrate that phosphorylation of LCD S269 and T291 by AKT can disrupt HIP-55 self-association and further prevent and reverse HIP-55 phase separation.

β-AR Hyperactivation Stress Reduces HIP-55 Phosphorylation and Boosts HIP-55 Abnormal Phase Separation and Insoluble Aggregation

Next, we sought to investigate the functional significance of HIP-55 LLPS and its regulation by phosphorylation in HF progression. We conducted an isoproterenol long-term treated cardiomyocyte model. We found that the HIP-55 S269 and T291 phosphorylation levels in isolated primary cardiomyocytes were significantly decreased with isoproterenol treatment (Figure 6A). Accompanied by the decreased phosphorylation, isoproterenol treatment also dramatically induced excessive abnormal phase separation of both endogenous HIP-55 (Figure 6B) in primary cardiomyocytes and exogenous HIP-55 in NIH-3T3 cells (Figure 6C).

Furthermore, immunohistochemical analysis showed that HIP-55 forms more aggregates in HF tissue (Figure 6D). This observation was supported by our finding that insoluble HIP-55 is significantly increased in both isoproterenol-treated cardiomyocytes and HF mice (Figure 6E and 6F).

Given the pathological relevance of insoluble HIP-55, we further examined the formation of the insoluble fraction during HIP-55 phase separation and AKT phosphorylation in cells. We overexpressed HIP-55WT and the phase separation–deficient mutant HIP-55R/A in NIH-3T3 cells. Compared with HIP-55WT, the insoluble fraction of HIP-55R/A was significantly diminished (Figure 6G). Even upon long-term isoproterenol treatment, which dramatically induced the formation of an HIP-55WT insoluble fraction, HIP-55R/A hardly formed any insoluble fraction (Figure 6H). These results demonstrated the direct link between HIP-55 phase separation and insoluble fraction formation.

Furthermore, we examined AKT-mediated HIP-55 phosphorylation in regulating HIP-55 insoluble fraction formation. Knockdown of AKT or AKT inhibitor MK2206 treatment, which promoted HIP-55 phase separation (Figure 5D through 5E), remarkably boosted the formation of HIP-55 insoluble fraction in NIH-3T3 cells (Figure 6I and 6J). We further confirmed these findings in primary cardiomyocytes. The isoproterenol treatment significantly decreased phosphorylation of HIP-55WT S269/T291 sites in primary cardiomyocytes (Figure 6K), which led to HIP-55 excessive phase separation and insoluble aggregation (Figure 6L and 6M). Meanwhile, AKT phosphorylation-deficient HIP-55AA formed a much more insoluble fraction compared with HIP-55WT in cardiomyocytes upon isoproterenol treatment (Figure 6K through 6M). These data illustrate that HIP-55 S269/T291 phosphorylation regulates phase separation and insoluble aggregation.

Therefore, β-AR hyperactivation stress reduces HIP-55 phosphorylation and boosts HIP-55 abnormal phase separation and insoluble aggregation.

Dynamic LLPS of HIP-55 is Necessary for Inhibiting the β-AR Downstream P38/MAPK HF Pathway

We next investigated how dynamic LLPS of HIP-55 regulates β-AR–mediated HF. It is well known that P38/MAPK plays a key role in β-AR–mediated HF.[16] We showed that deficiency of HIP-55 significantly activated the cardiac β-AR–mediated P38/MAPK pathway (Figure 7A). In contrast, compared with WT mice, cardiac-specific overexpression of HIP-55 remarkably decreased the β-AR–mediated P38/MAPK pathway (Figure 7B). Moreover, knockdown of HIP-55 increased β-AR–mediated P38/MAPK activation, and overexpression of HIP-55 significantly inhibited the β-AR–mediated P38/MAPK pathway both in HEK-293A cells and primary cardiomyocytes (Figure 7C through 7F). These in vivo and in vitro results indicate that HIP-55 negatively regulates β-AR–mediated P38/MAPK activation.

Furthermore, compared with overexpression of HIP-55WT, overexpression of HIP-55R/A or HIP-55AA

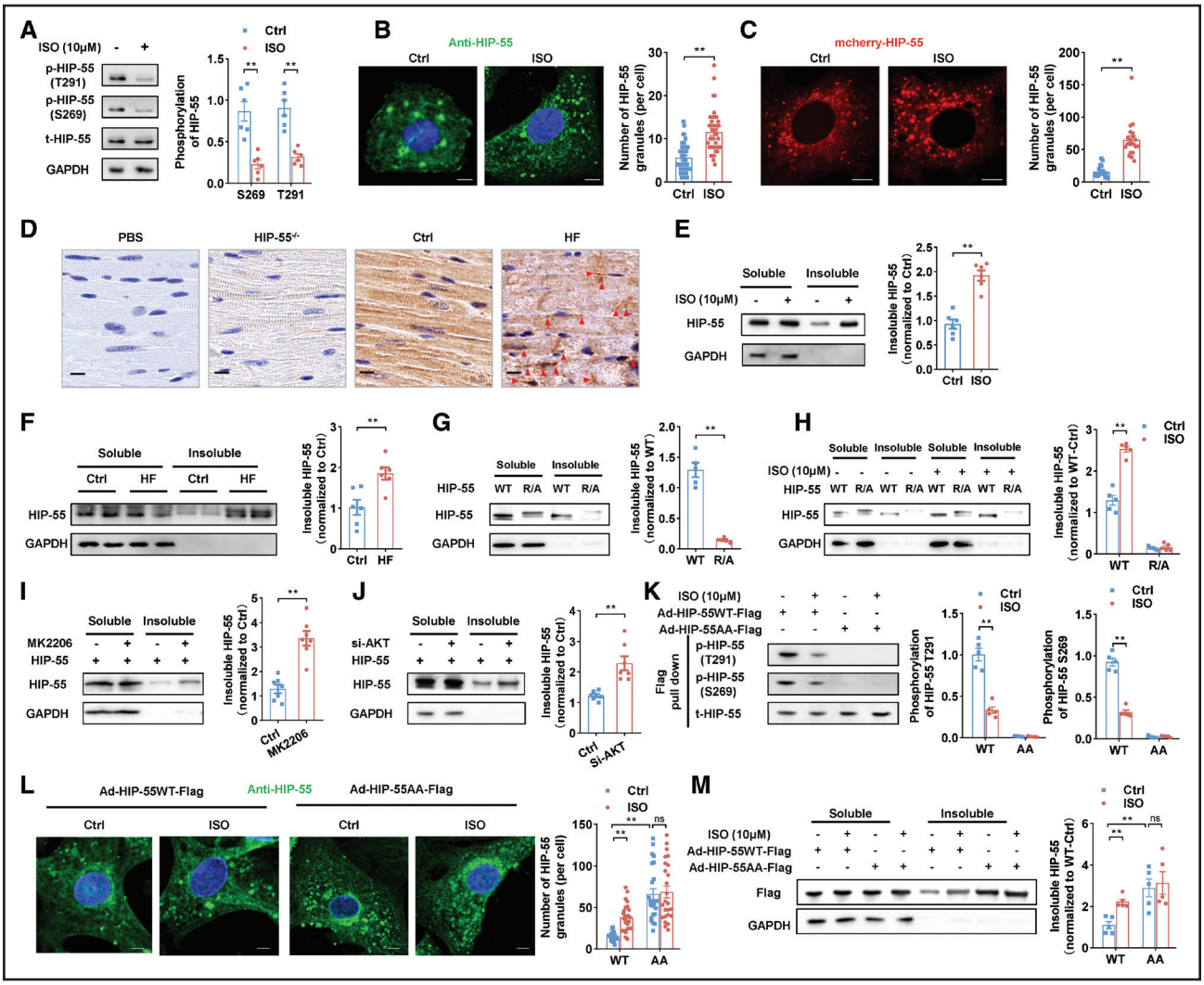

Figure 6. β-AR hyperactivation stress reduces HIP-55 phosphorylation and boosts HIP-55 abnormal phase separation and insoluble aggregation.

A, Primary cardiomyocytes were treated with isoproterenol (ISO; 10 μM) for 48 hours. The phosphorylation of endogenous HIP-55 (hematopoietic progenitor kinase 1–interacting protein of 55 kDa) was detected by the p-HIP-55 (S269) and p-HIP-55 (T291) antibodies (n=5). **B**, Primary cardiomyocytes were treated with ISO (10 μM) for 48 hours. Endogenous HIP-55 immunofluorescence was then detected by anti–HIP-55 antibodies (dilution, 1:200). Scale bar=5 μm (n=40). **C**, NIH-3T3 cells were transfected with mCherry–HIP-55 plasmids and then treated with ISO (10 μM) for 48 hours. Scale bar=5 μm (n=20). **D**, Immunohistochemistry staining of endogenous HIP-55 using anti–HIP-55 antibodies (dilution, 1:200) in normal heart tissue and heart failure (HF) tissue. Incubation with PBS instead of anti–HIP-55 antibodies was used as negative control. Incubation with anti–HIP-55 antibodies in HIP-55$^{-/-}$ mice was used to confirm the specificity of the HIP-55 antibody. Arrows indicate aggregates. Scale bar=10 μm (n=6). **E**, Primary cardiomyocytes were treated with ISO (10 μM for 48 hours). Insoluble HIP-55 was then detected by Western blot (n=5). **F**, Detection of insoluble HIP-55 in heart tissue from heart failure mice (n=6). **G**, NIH-3T3 cells were transfected with mCherry–HIP-55 plasmids as indicated. Insoluble HIP-55 was then detected by Western blot (n=5). **H**, NIH-3T3 cells were transfected with mCherry–HIP-55 plasmids as indicated and treated with ISO (10 μM) for 48 hours. Insoluble HIP-55 was then detected by Western blot (n=5). **I**, NIH-3T3 cells were transfected with mCherry–HIP-55 plasmids and treated with MK2206 (5 μM) for 48 hours. Insoluble HIP-55 was then detected by Western blot (n=7). **J**, NIH-3T3 cells were transfected with mCherry–HIP-55 plasmids or siRNA of AKT as indicated. The insoluble HIP-55 was then detected by Western blot (n=7). **K**, Primary cardiomyocytes were infected with adenovirus vectors that carry Flag-tagged HIP-55WT (Ad-HIP-55WT-Flag) or HIP-55AA (Ad-HIP-55AA-Flag) genes. Then, these cardiomyocytes were treated with ISO (10 μM) for 48 hours. Flag-tagged HIP-55 was enriched by Flag pull down and then detected by the p-HIP-55 (S269) and p-HIP-55 (T291) antibodies (n=5). **L**, Primary cardiomyocytes were infected and treated as indicated in **K**. The exogenous HIP-55 immunofluorescence was detected by anti–HIP-55 antibodies (dilution, 1:1000). Scale bar=5 μm (n=25). **M**, The primary cardiomyocytes were infected with adenovirus vectors as indicated and treated with ISO (10 μM) for 48 hours. The exogenous insoluble HIP-55 was then detected by Western blot (n=5). Statistical analyses were performed by unpaired *t* test (**A**, **E**, **F**, **G**, **I**, **J**, and **K**: phosphorylation of HIP-55 T291), the Mann-Whitney *U* test (**B**, **C**, and **K**: phosphorylation of HIP-55 S269), 2-way ANOVA followed by Bonferroni post hoc correction (**H** and **M**), and the Kruskal-Wallis test followed by the Dunn post hoc test (**L**). **P*<0.05, ***P*<0.01.

ORIGINAL RESEARCH ARTICLE

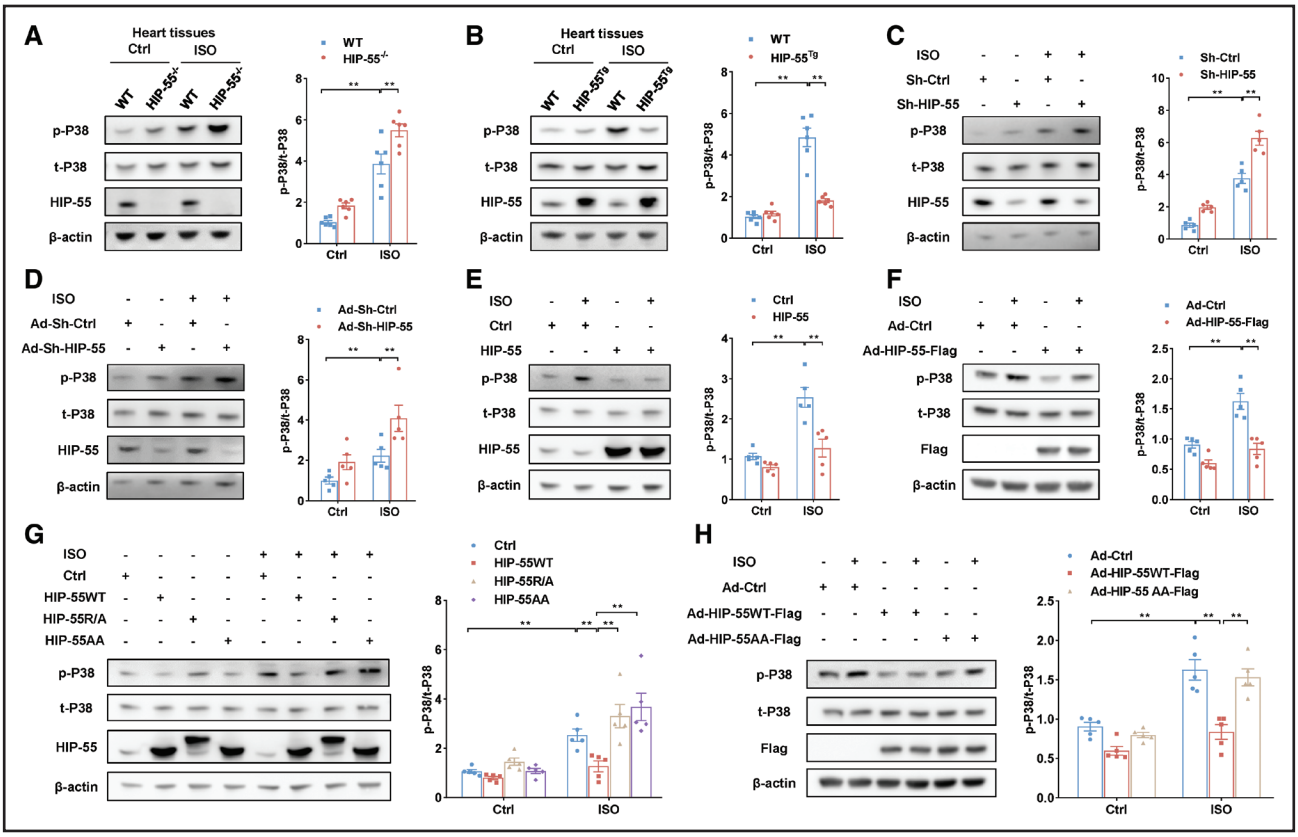

Figure 7. Dynamic liquid–liquid phase separation of HIP-55 is necessary for inhibiting the β-adrenergic receptor downstream P38/MAPK heart failure pathway.

A, Representative immunoblots and statistical analysis of P38/MAPK (mitogen-activated protein kinase) activation in wild-type (WT) and HIP-55$^{-/-}$ mouse hearts after 4 weeks of isoproterenol (ISO) treatment (n=6). **B**, Representative immunoblots and statistical analysis of P38/MAPK activation in WT and HIP-55^{Tg} mouse hearts after ISO treatment (n=6). **C**, HEK-293A cells were transfected with plasmids that carry either short hairpin RNA (shRNA) targeting human HIP-55 (hematopoietic progenitor kinase 1–interacting protein of 55 kDa; Sh-HIP-55) or scrambled control (Sh-Ctrl). Cells were then treated with ISO (10 μM) for 10 minutes, and P38 activation was analyzed by Western blot (n=5). **D**, Primary cardiomyocytes were infected with adenovirus vectors that carry either shRNA targeting mouse HIP-55 (Ad-Sh-HIP-55) or scrambled control (Ad-Sh-Ctrl). Cardiomyocytes were then treated with ISO (10 μM) for 10 minutes, and P38/MAPK activation was analyzed by Western blot (n=5). **E**, HEK-293A cells were transfected with HIP-55 or control plasmids. Cells were then treated with ISO (10 μM) for 10 minutes, and P38/MAPK activation was analyzed by Western blot (n=5). **F**, Primary cardiomyocytes were infected with adenovirus vectors that carry Flag-tagged HIP-55 (Ad-HIP-55) genes. Cardiomyocytes were then treated with ISO (10 μM) for 10 minutes, and P38/MAPK activation was analyzed by Western blot (n=5). **G**, HIP-55 inhibited ISO-induced P38/MAPK activation by means of dynamic phase separation. HEK-293A cells were transfected with HIP-55WT (with dynamic liquid–liquid phase separation [LLPS]), HIP-55R/A (with deficient LLPS), and HIP-55AA (with abnormal LLPS) plasmids. Cells were then treated with ISO (10 μM) for 10 minutes, and P38/MAPK activation was analyzed by Western blot (n=5). **H**, HIP-55 inhibited ISO-induced P38/MAPK activation by means of its dynamic phase separation. Primary cardiomyocytes were infected with adenovirus vectors that carried either Flag-tagged HIP-55WT (Ad-HIP-55WT-Flag) or HIP-55AA (Ad-HIP-55AA-Flag), and P38/MAPK activation was analyzed by Western blot (n=5). Statistical analyses were performed by 2-way ANOVA followed by Bonferroni post hoc correction (**A** through **H**). $^{**}P<0.01$.

reduces their inhibitory effects on β-AR–mediated P38/MAPK activation (Figure 7G). In primary cardiomyocytes, we also found that overexpression of HIP-55AA cannot inhibit β-AR–mediated P38/MAPK activation (Figure 7H).

Taken together, these results indicated that HIP-55 protects against HF by the dynamic regulation of HIP-55 LLPS of the β-AR downstream P38/MAPK HF pathway.

Dysregulated Phase Separation of HIP-55 Abolishes Its Protective Function Against HF

To provide further evidence in an animal HF model, we developed cardiac-specific overexpressed HIP-55AA transgenic mice (HIP-55AA^{Tg}; Figure 8A and 8B). The cardiac-specific transgenic and control mice underwent isoproterenol-induced HF as described previously. Immunohistochemical detection revealed that under β-AR overactivation, the cardiac-specific overexpressed HIP-5AA formed more aggregate-like structures in heart tissue than in cardiac-specific overexpressed HIP-55WT mice (Figure 8C). Cardiac-specific overexpression of HIP-55WT, but not HIP-55AA, consistently significantly inhibited the β-AR–mediated P38/MAPK HF pathway (Figure 8D). Moreover, compared with control mice, cardiac-specific overexpression of HIP-55WT, but not HIP-55AA, significantly improved cardiac systolic function after long-term sympathetic hyperactivation stress stimulation (Figure 8E; Table S2). HIP-55WT^{Tg} mice

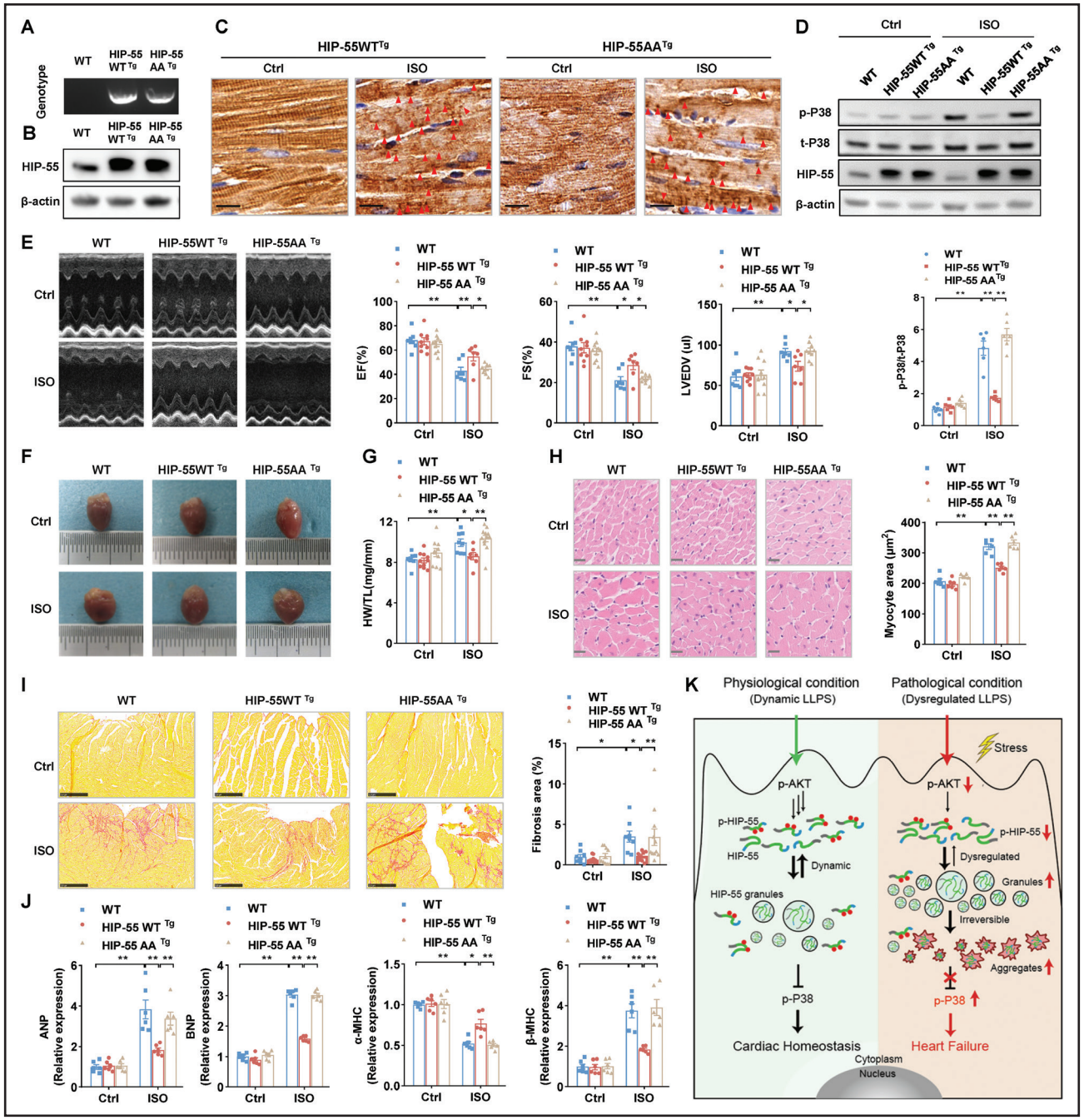

Figure 8. Dysregulated phase separation of HIP-55 abolishes its protective function against heart failure.
A, Genotypes of wild-type (WT), HIP-55WT^{Tg}, and HIP-55AA^{Tg} mice. **B**, Detection of HIP-55 (hematopoietic progenitor kinase 1–interacting protein of 55 kDa) expression in heart tissue from WT, HIP-55WT^{Tg}, and HIP-55AA^{Tg} mice. **C**, Immunohistochemistry staining of HIP-55 using anti–HIP-55 antibodies (dilution, 1:800) in heart tissue from control or isoproterenol (ISO)–treated transgenic mice. Arrows indicate aggregates. Scale bar=10 μm (n=6). **D**, Analysis of long-term ISO-induced P38 activation in heart tissue from WT, HIP-55WT^{Tg}, and HIP-55AA^{Tg} mice (n=6). **E**, Representative M-mode echocardiographic imaging of heart and cardiac function analysis of ejection fraction (EF%), fractional shortening (FS%), and left ventricular end diastolic volume (LVEDV) after 4 weeks of ISO treatment (n=7–10). **F**, Gross view of WT, HIP-55WT^{Tg}, and HIP-55AA^{Tg} mouse heart tissue after saline or ISO treatment for 4 weeks. **G**, The ratio of heart weight to tibial length (HW/TL) in WT, HIP-55WT^{Tg}, and HIP-55AA^{Tg} mice (n=7–12). **H**, Hematoxylin & eosin staining micrographs of cross-sections of myocardia. Scale bar=20 μm (n=6). **I**, Representative photograph of Sirius red staining and quantification of fibrotic areas. Scale bar=250 μm (n=8–11). **J**, Detection of mRNA levels of heart failure marker genes (*ANP*, *BNP*, *α-MHC*, and *β-MHC*) in heart tissue from WT, HIP-55WT^{Tg}, and HIP-55AA^{Tg} mice after ISO treatment (n=6). **K**, Working model showing phosphorylation-regulated dynamic phase separation of HIP-55 is necessary for protection against heart failure. HIP-55 possesses a strong capacity for phase separation that is dynamically regulated by AKT-mediated phosphorylation on S269/T291 in the low-complexity domain. Under physiological conditions, HIP-55 phase separation is in a dynamic equilibrium to maintain homeostasis of β-AR–mediated P38/MAPK signaling pathway activation in the heart. Under pathological conditions, prolonged excessive sympathetic hyperactivation decreases HIP-55 phosphorylation. In accordance, HIP-55 tends to form massive granules and insoluble aggregates, impairing its protective activity against heart failure. Statistical analyses were performed by 2-way ANOVA followed by Bonferroni post hoc correction (**D**, **E**, **G**, **H**, **I**, and **J**). *P<0.05, **P<0.01.

showed less adverse cardiac hypertrophy and fibrosis, whereas HIP-55AA^{Tg} mice showed diminished amelioration (Figure 8F through 8I). The cardiac-dysfunction marker gene expression, such as the *ANP*, *BNP*, and *MHC* isoform switch, was also dramatically inhibited in the hearts of HIP-55WT^{Tg} mice, but not HIP55AA^{Tg} mice (Figure 8J). Thus, these results showed that phosphorylation-deficient HIP-55AA, with loss of dynamic LLPS, loses its protective function against HF, which indicates the critical role of dynamic HIP-55 LLPS in HF progression (Figure 8K).

DISCUSSION

HF is an elusive syndrome, and its pathogenesis and mechanisms are complicated. Protein phase separation recently has been found to play an essential role in a variety of different physical and pathological processes.[7,15] However, protein phase separation has not yet been linked to HF. In this study, we demonstrate that HIP-55 functions as a key modulator of HF through phase separation. We demonstrate that dynamic phase separation of HIP-55, which is intricately regulated by its S269/T291 phosphorylation, is critical in inhibiting hyperactivation of the β-AR signaling pathway. Under long-term sympathetic hyperactivation stress, HIP-55 phosphorylation is diminished, which significantly promotes abnormal phase separation and eliminates the protective activity of HIP-55 against aberrant β-AR–mediated signaling in HF.

HIP-55 possesses the known structural characteristics required for phase separation. Our sequence analysis shows that HIP-55 is characterized by a highly flexible and long LCD. Numerous proteins containing LCDs are able to undergo LLPS and engage in the assembly of functional membrane-less organelles.[7] It has been suggested that LCDs are crucial in driving protein phase separation by means of weak and transient self-association interactions.[7] Our molecular mechanistic study revealed that HIP-55 phase separation is driven by electrostatic interaction within its LCD. Our cellular fluorescence recovery after photobleaching assay and fractionated cell lysate assay indicate that the interior mobility of HIP-55 is less dynamic in a granule form as compared with the other well-known, highly dynamic granules, such as stress granules,[17] implying that HIP-55 granules exhibit limited internal dynamics and are prone to form insoluble aggregates in cells, especially under disease conditions. Previous studies showed that LCDs of several proteins related to neurodegenerative diseases, including FUS (fused in sarcoma), hnRNPA1 (heterogeneous nuclear ribonucleoprotein A1), and TDP-43 (TAR DNA-binding protein 43), are prone to phase separate to fulfill physiological functions, but undergo transitions to form solid-like aggregations from liquid-like granules under disease conditions.[15] Compositional bias analysis shows that Gln, which is enriched in the FUS LCD and was identified to be important in promoting the hardening process of FUS-containing granules,[18] is also highly enriched in the HIP-55 LCD. Thus, it is possible that a high proportion of Gln residue within the HIP-55 LCD renders a highly concentrated HIP-55 prone to promote insoluble aggregations of HIP-55 granules. However, further study is needed to investigate the molecular basis of HIP-55 aggregation under disease conditions.

Our work demonstrates that dynamic phase separation of proteins may play a previously unappreciated and important role in HF. It seems reasonable to speculate that dysregulation of protein phase separation might broadly participate in pathophysiological processes within the cardiovascular system. On the one hand, the cardiovascular system, including the heart and vasculature, is constantly exposed to different stresses, including blood pressure changes, cardiac electrical activity, and adrenergic stimulation, among others. Because protein phase separation was originally defined as mediating stress granule formation,[19] it is plausible that cardiovascular stress may induce phase separation of different proteins participating in different pathophysiological processes within the cardiovascular system. On the other hand, abnormal or accumulated protein aggregation recently has been detected in aged or diseased hearts, such as in idiopathic or ischemic cardiomyopathy, arrhythmia, and HF.[20–23] It is possible that the numerous cardiac aggregations in heart diseases might be related to dysregulation of protein phase separation under different disease conditions. Further in-depth studies are needed to decipher the role of protein phase separation and aggregation in different cardiac diseases.

As a signaling adaptor protein, HIP-55 regulates various signaling pathways, depending upon its own regulated function. P38/MAPK kinase, also known as stress-activated protein kinase, is a type of evolutionarily conserved serine/threonine MAPK that plays key roles in cardiac hypertrophy, fibrosis, inflammation, and cardiomyocyte death.[6,24,25] Numerous studies have shown that cardiac pathological stimuli, such as ischemia, pressure overload, and sympathetic hyperactivation, lead to P38/MAPK pathway overactivation.[25] Inhibiting P38/MAPK overactivation significantly alleviates adverse cardiac remodeling and HF progression.[6,16] Here, we demonstrate that HIP-55 operates as an inherent regulator to maintain the homeostasis of β-AR–mediated P38/MAPK signaling pathway activation in the heart. The phosphorylation-regulated dynamic LLPS of HIP-55 controls the β-AR downstream P38/MAPK HF pathway. Prolonged excessive sympathetic hyperactivation decreased HIP-55 phosphorylation, resulting in abnormal HIP-55 LLPS and overactivation of P38/MAPK and ultimately contributing to HF.

Our work links prolonged sympathetic hyperactivation-induced dysregulated protein phase separation to HF, and offers new insight into the mechanism of HF. This novel mechanism also reveals that restoring the dynamic phase separation of HIP-55 may provide a new strategy for developing innovative therapies for HF.

ARTICLE INFORMATION

Received October 16, 2023; accepted January 5, 2024.

Affiliations

Department of Cardiology and Institute of Vascular Medicine (Y.J., X.N., Y.Z., Y.T., Z.L.) and Department of Pharmacy (Z.L.), Peking University Third Hospital, Beijing, China. Beijing Key Laboratory of Cardiovascular Receptors Research, State Key Laboratory of Vascular Homeostasis and Remodeling, and NHC Key Laboratory of Cardiovascular Molecular Biology and Regulatory Peptides, Peking University, Beijing, China (Y.J., X.N., Y.Z., Y.T., Z.L.). Research Unit of Medical Science Research Management/Basic and Clinical Research of Metabolic Cardiovascular Diseases, Chinese Academy of Medical Sciences, Beijing, China (Y.J., X.N., Y.Z., Y.T., Z.L.). Interdisciplinary Research Center on Biology and Chemistry and State Key Laboratory of Chemical Biology, Shanghai Institute of Organic Chemistry, Chinese Academy of Sciences, Shanghai, China (J.G., J.H., C.L.). Bio-X Institutes, Key Laboratory for the Genetics of Developmental and Neuropsychiatric Disorders (Ministry of Education), Shanghai Jiao Tong University, Shanghai, China (D.L.).

Sources of Funding

This work was supported by the National Key Research and Development Program of China (grant 2022YFC3602400), the National Natural Science Foundation of China (grants U21A20336, 81820108031, and 91939301), the Beijing Municipal Natural Science Foundation (grant 7222218), and the CAMS Innovation Fund for Medical Sciences (grant 2021-I2M-5-003) to Dr Li; the National Natural Science Foundation of China (grants 82188101, 32170683, and 32171236), the Science and Technology Commission of Shanghai Municipality (grants 20XD1425000, 2019SHZDZX02, and 22JC1410400), and the Shanghai Pilot Program for Basic Research–Chinese Academy of Science, Shanghai Branch (grant CYJ-SHFY-2022-005) to Dr Liu; the National Natural Science Foundation of China (grant 82200378), the Beijing Municipal Natural Science Foundation (grant 7224349), the Postdoctoral Fellowship of Peking-Tsinghua Center for Life Sciences, the China Postdoctoral Science Foundation (grant 2021M700275), and the Peking University Medicine Fund of Fostering Young Scholars' Scientific & Technological Innovation to Dr Jiang.

Disclosures

None.

Supplemental Material

Methods

Tables S1–S2

REFERENCES

1. Taylor CJ, Ordóñez-Mena JM, Roalfe AK, Lay-Flurrie S, Jones NR, Marshall T, Hobbs FDR. Trends in survival after a diagnosis of heart failure in the United Kingdom 2000-2017: population based cohort study. *BMJ*. 2019;364:l223. doi: 10.1136/bmj.l223
2. Triposkiadis F, Karayannis G, Giamouzis G, Skoularigis J, Louridas G, Butler J. The sympathetic nervous system in heart failure physiology, pathophysiology, and clinical implications. *J Am Coll Cardiol*. 2009;54:1747–1762. doi: 10.1016/j.jacc.2009.05.015
3. Zheng M, Zhu W, Han Q, Xiao RP. Emerging concepts and therapeutic implications of beta-adrenergic receptor subtype signaling. *Pharmacol Ther*. 2005;108:257–268. doi: 10.1016/j.pharmthera.2005.04.006
4. Kim J, Eckhart AD, Eguchi S, Koch WJ. Beta-adrenergic receptor-mediated DNA synthesis in cardiac fibroblasts is dependent on transactivation of the epidermal growth factor receptor and subsequent activation of extracellular signal-regulated kinases. *J Biol Chem*. 2002;277:32116–32123. doi: 10.1074/jbc.M204895200
5. Liu N, Xing R, Yang C, Tian A, Lv Z, Sun N, Gao X, Zhang Y, Li Z. HIP-55/DBNL-dependent regulation of adrenergic receptor mediates the ERK1/2 proliferative pathway. *Mol Biosyst*. 2014;10:1932–1939. doi: 10.1039/c3mb70525k
6. Yin Q, Lu H, Bai Y, Tian A, Yang Q, Wu J, Yang C, Fan TP, Zhang Y, Zheng X, et al. A metabolite of Danshen formulae attenuates cardiac fibrosis induced by isoprenaline, via a NOX2/ROS/p38 pathway. *Br J Pharmacol*. 2015;172:5573–5585. doi: 10.1111/bph.13133
7. Banani SF, Lee HO, Hyman AA, Rosen MK. Biomolecular condensates: organizers of cellular biochemistry. *Nat Rev Mol Cell Biol*. 2017;18:285–298. doi: 10.1038/nrm.2017.7
8. Su X, Ditlev JA, Hui E, Xing W, Banjade S, Okrut J, King DS, Taunton J, Rosen MK, Vale RD. Phase separation of signaling molecules promotes T cell receptor signal transduction. *Science*. 2016;352:595–599. doi: 10.1126/science.aad9964
9. Boija A, Klein IA, Sabari BR, Dall'Agnese A, Coffey EL, Zamudio AV, Li CH, Shrinivas K, Manteiga JC, Hannett NM, et al. Transcription factors activate genes through the phase-separation capacity of their activation domains. *Cell*. 2018;175:1842–1855.e16. doi: 10.1016/j.cell.2018.10.042
10. Gibson BA, Doolittle LK, Schneider MWG, Jensen LE, Gamarra N, Henry L, Gerlich DW, Redding S, Rosen MK. Organization of chromatin by intrinsic and regulated phase separation. *Cell*. 2019;179:470–484.e21. doi: 10.1016/j.cell.2019.08.037
11. Zhang H, Ji X, Li P, Liu C, Lou J, Wang Z, Wen W, Xiao Y, Zhang M, Zhu X. Liquid-liquid phase separation in biology: mechanisms, physiological functions and human diseases. *Sci China Life Sci*. 2020;63:953–985. doi: 10.1007/s11427-020-1702-x
12. Schymeinsky J, Sperandio M, Walzog B. The mammalian actin-binding protein 1 (mAbp1): a novel molecular player in leukocyte biology. *Trends Cell Biol*. 2011;21:247–255. doi: 10.1016/j.tcb.2010.12.001
13. Jiang Y, Qiao Y, He D, Tian A, Li Z. Adaptor protein HIP-55-mediated signalosome protects against ferroptosis in myocardial infarction. *Cell Death Differ*. 2023;30:825–838. doi: 10.1038/s41418-022-01110-z
14. Wegmann S, Eftekharzadeh B, Tepper K, Zoltowska KM, Bennett RE, Dujardin S, Laskowski PR, MacKenzie D, Kamath T, Commins C, et al. Tau protein liquid–liquid phase separation can initiate tau aggregation. *EMBO J*. 2018;37:e98049. doi: 10.15252/embj.201798049
15. Alberti S, Dormann D. Liquid-liquid phase separation in disease. *Annu Rev Genet*. 2019;53:171–194. doi: 10.1146/annurev-genet-112618-043527
16. Behr TM, Nerurkar SS, Nelson AH, Coatney RW, Woods TN, Sulpizio A, Chandra S, Brooks DP, Kumar S, Lee JC, et al. Hypertensive end-organ damage and premature mortality are p38 mitogen-activated protein kinase-dependent in a rat model of cardiac hypertrophy and dysfunction. *Circulation*. 2001;104:1292–1298. doi: 10.1161/hc3601.094275
17. Lee KH, Zhang P, Kim HJ, Mitrea DM, Sarkar M, Freibaum BD, Cika J, Coughlin M, Messing J, Molliex A, et al. C9orf72 dipeptide repeats impair the assembly, dynamics, and function of membrane-less organelles. *Cell*. 2016;167:774–788.e17. doi: 10.1016/j.cell.2016.10.002
18. Wang J, Choi JM, Holehouse AS, Lee HO, Zhang X, Jahnel M, Maharana S, Lemaitre R, Pozniakovsky A, Drechsel D, et al. A molecular grammar governing the driving forces for phase separation of prion-like RNA binding proteins. *Cell*. 2018;174:688–699.e16. doi: 10.1016/j.cell.2018.06.006
19. Molliex A, Temirov J, Lee J, Coughlin M, Kanagaraj AP, Kim HJ, Mittag T, Taylor JP. Phase separation by low complexity domains promotes stress granule assembly and drives pathological fibrillization. *Cell*. 2015;163:123–133. doi: 10.1016/j.cell.2015.09.015
20. Tannous P, Zhu H, Nemchenko A, Berry JM, Johnstone JL, Shelton JM, Miller FJ Jr, Rothermel BA, Hill JA. Intracellular protein aggregation is a proximal trigger of cardiomyocyte autophagy. *Circulation*. 2008;117:3070–3078. doi: 10.1161/CIRCULATIONAHA.107.763870
21. Ayyadevara S, Mercanti F, Wang X, Mackintosh SG, Tackett AJ, Prayaga SV, Romeo F, Shmookler Reis RJ, Mehta JL. Age- and hypertension-associated protein aggregates in mouse heart have similar proteomic profiles. *Hypertension*. 2016;67:1006–1013. doi: 10.1161/HYPERTENSIONAHA.115.06849
22. Selcen D, Ohno K, Engel AG. Myofibrillar myopathy: clinical, morphological and genetic studies in 63 patients. *Brain*. 2004;127:439–451. doi: 10.1093/brain/awh052
23. Henning RH, Brundel BJJM. Proteostasis in cardiac health and disease. *Nat Rev Cardiol*. 2017;14:637–653. doi: 10.1038/nrcardio.2017.89
24. Tenhunen O, Rysä J, Ilves M, Soini Y, Ruskoaho H, Leskinen H. Identification of cell cycle regulatory and inflammatory genes as predominant targets of p38 mitogen-activated protein kinase in the heart. *Circ Res*. 2006;99:485–493. doi: 10.1161/01.RES.0000238387.85144.92
25. Rose BA, Force T, Wang Y. Mitogen-activated protein kinase signaling in the heart: angels versus demons in a heart-breaking tale. *Physiol Rev*. 2010;90:1507–1546. doi: 10.1152/physrev.00054.2009